Radio Science, Volume 22, Number 6, Pages 1109–1116, November 1987

Measuring and modeling the backscattering cross section of a leaf

T. B. A. Senior, K. Sarabandi, and F. T. Ulaby

Radiation Laboratory, Electrical Engineering and Computer Science Department, University of Michigan, Ann Arbor

(Received February 25, 1987; revised June 15, 1987; accepted June 17, 1987.)

Leaves are a significant feature of any vegetation canopy, and for remote sensing purposes it is important to develop an effective model for predicting the scattering from a leaf. From measurements of the X band backscattering cross section of a coleus leaf in varying stages of dryness, it is shown that a uniform resistive sheet constitutes such a model for a planar leaf. The scattering is determined by the (complex) resistivity which is, in turn, entirely specified by the gravimetric moisture content of the leaf. Using an available asymptotic expression for the scattering from a rectangular resistive plate which includes, as a special case, a metallic plate whose resistivity is zero, the computed backscattering cross sections for both principal polarizations are found to be in excellent agreement with data measured for rectangular sections of leaves with different moisture contents. If the resistivity is sufficiently large, the asymptotic expressions do not differ significantly from the physical optics ones, and for naturally shaped leaves as well as rectangular sections, the physical optics approximation in conjunction with the resistive sheet model faithfully reproduces the dominant features of the scattering patterns under all moisture conditions.

1. INTRODUCTION

At centimeter wavelengths, a vegetation canopy consists of scatterers with sizes that span a wide range of values extending from a fraction of a wavelength to several wavelengths. The scattering and extinction properties of an individual scatterer are governed by its shape, size, orientation, and dielectric properties. For purposes of modeling the backscattering from a forest canopy, the canopy is often treated as an inhomogeneous layer containing sparsely distributed, randomly positioned discrete scatterers [*Lang*, 1981; *Levine et al.*, 1983, 1985; *Tsang et al.*, 1984]. The sizes, shapes and orientation of the scatterers are specified by probability density functions.

Leaves are a major constituent of many types of plants, and a knowledge of their scattering and extinction properties is very important in microwave remote sensing. Although most leaves are irregular in shape and are not flat, they are often modeled as flat circular discs with known radius, thickness, and dielectric constant [*Levine et al.*, 1983, 1985]. This brings up the following set of fundamental questions:

1. What formulation might one use to characterize the backscattering and extinction cross sections of a regularly shaped (elliptical or rectangular) flat leaf?
2. How does one relate the radar cross section σ to the leaf moisture content Mg?
3. Is it possible to approximate the scattering and extinction cross sections of a flat irregularly shaped leaf using the formulations for a rectangular leaf of equal physical area?
4. What is the effect of leaf curvature on its scattering behavior?

In this paper we shall address the first two questions by proposing a resistive sheet model and verifying the model with experimental measurements conducted for sections of leaves (all cut in the shape of a rectangle) at various levels of moisture content, and partially examine the third question by comparing the scattering pattern calculated for a rectangular plate with measurements obtained for an irregularly shaped leaf. Exploration of the effects of leaf curvature will be the subject of future work.

2. EXPERIMENTAL PROCEDURE

The radar cross section (RCS) measurements reported in this paper were made at 10 GHz using a small rectangular horn antenna connected to a HP 8510A network analyzer, as illustrated by the sketch in Figure 1. The horn antenna, whose aperture mea-

Paper number 7S0540.
0048-6604/87/007S-0540$08.00

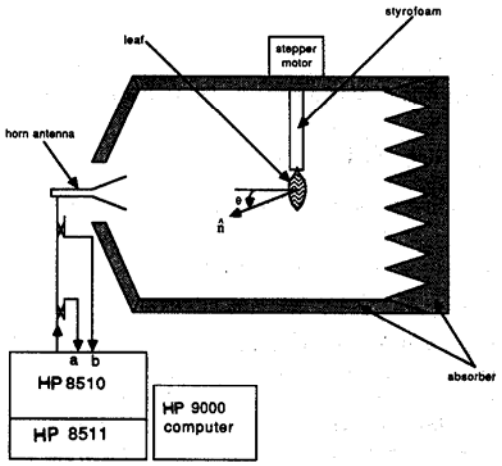

Fig. 1. Schematic of the RCS measurement system.

sured 6 cm × 6 cm, was located at the throat of a small anechoic chamber, and the leaf was suspended from the top by a thin styrofoam cylinder. The center of the top edge of the leaf was glued to the styrofoam cylinder which could be rotated to any angle θ between the backscattered direction and the normal to the plane of the leaf.

2.1. *System sensitivity and calibration*

The HP 8510A is a vector network analyzer capable of measuring both the amplitude and phase of the reflected signal (channel b in Figure 1) relative to a sample of the transmitted signal (channel a in Figure 1). To enhance the measurement sensitivity of the system, two measurements are made: one for the background alone, which includes the styrofoam cylinder, and another with the target present. By subtracting the complex signal recorded for the background alone from that measured in the presence of the target, significant improvement is obtained in the target-to-background ratio.

Absolute calibration of the system was achieved by measuring the cross section σ of a metal sphere. According to these measurements, the noise-equivalent σ of the system is about -80 dBsm. Consequently, in most cases only data above -60 dBsm was recorded, which corresponds to a target-to-background ratio of 20 dB or greater.

To test the linearity of the system and establish the extent of its dynamic range, RCS measurements were performed for seven metal spheres with diameters from 0.79 cm to 3.81 cm. The largest sphere was used to calibrate the system and the other six were used to evaluate the system accuracy by comparing the measured RCS with theoretical values computed from the Mie series. The continuous curve in Figure 2 is a plot of σ/λ^2 as a function of D/λ for a perfectly conducting sphere of diameter D, and the "stars" represent the measured data. The rms error, computed for the six test spheres, is 0.33 dB.

2.2. *Leaf moisture and dielectric constant*

The leaf moisture content was determined by measuring its weight immediately after measuring its RCS, and once again at the conclusion of the experiment. The latter measurement was made after drying the leaf in an oven at 70°C until equilibrium was reached. The difference in weight represents the weight of liquid water that was present in the leaf when its RCS was measured. The gravimetric moisture content Mg is the weight fraction of water in the leaf to the total weight.

Using the data measured and the models developed by *Ulaby and El-Rayes* [1986] for the dielectric constant of vegetation, the following simple expressions were generated to characterize the relative dielectric constant ε at 10 GHz and room temperature ($T = 22$°C):

$$\begin{aligned} \varepsilon' &= 3.95 \exp(2.79\ \mathrm{Mg}) - 2.25 \\ \varepsilon'' &= 2.69 \exp(2.15\ \mathrm{Mg}) - 2.68 \end{aligned} \tag{1}$$

2.3. *Types of RCS measurements*

Two sets of RCS measurements were conducted. The first data set involved a leaf that had been cut in

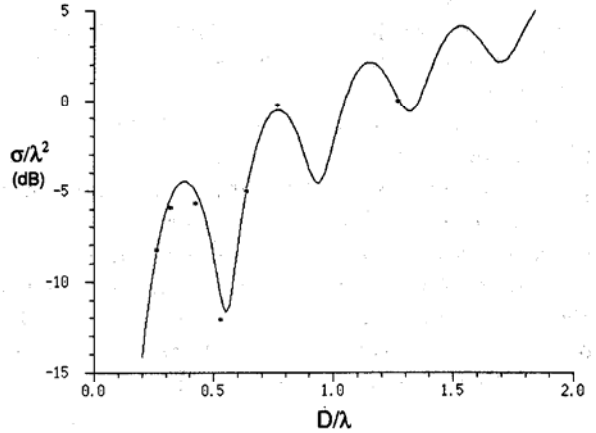

Fig. 2. The calibration accuracy and dynamic range of the measurement system were evaluated by comparing the measured RCS of metal spheres (asterisks) with theory.

the form of a rectangular plate 4 cm × 6 cm in area. With the long dimension oriented vertically, the cross section of the leaf was measured as a function of the angle of rotation θ about a vertical axis, with $\theta = 0$ corresponding to normal incidence. Each measurement scan consisted of σ versus θ in 5° steps from −90° to +90°. Usually, two scans were made, one with the antenna polarized with the electric vector vertical (E polarization) and the other with the magnetic vector vertical (H polarization). The first data set consisted of four pairs of scans corresponding to the rectangular leaf at Mg = 85% (freshly cut), 77% (a few hours later), 62% (a day later), and 0% (dry). The data comprising the second set are similar to those in the first except that the leaf was measured in its natural state without altering its shape. A profile is shown in the inset of Figure 7.

Maintaining the leaf flat to within a fraction of a wavelength was a consistent problem in this phase of the investigation, particularly for the "naturally" shaped leaf after it had been allowed to dry for a few days. Leaf thickness, which was measured using a micrometer, was found to decrease slowly with time after cutting as a result of shrinking due to loss of water. The variation of leaf thickness τ (mm) with Mg is given by the empirical expression

$$\tau = 0.032\ \mathrm{Mg}^2 + 0.091\ \mathrm{Mg} + 0.075 \tag{2}$$

In addition, it was observed that the drying took place from the outer edges of the leaf inwards, so that the moisture content was no longer uniform across the leaf.

3. THEORETICAL MODEL

3.1. *A resistive sheet*

A leaf can be viewed as a thin layer (of thickness τ) of a nonmagnetic dielectric material whose complex relative permittivity is ε, and a widely used model for such a layer is an infinitesimally thin resistive sheet whose resistivity is

$$R = \frac{iZ}{k\tau(\varepsilon - 1)} \tag{3}$$

ohms per square. In (3) k and $Z(=1/Y)$ are the propagation constant and intrinsic impedance, respectively, of the surrounding free space medium, and a time factor $e^{-i\omega t}$ has been assumed. When $R = 0$ the sheet appears perfectly conducting and when $R = \infty$ it ceases to exist.

The sheet is simply an electric current sheet whose strength is proportional to the local tangential electric field [*Harrington and Mautz*, 1975] via the single measurable quantity R. If n is the unit vector normal drawn outwards to the upper (positive) side of the sheet and $[\ ]_-^+$ denotes the discontinuity across the sheet, the boundary conditions are

$$[\hat{n} \times \bar{E}]_-^+ = 0 \tag{4}$$

implying continuity of the tangential electric field (a consequence of the absence of any magnetic current), and

$$\hat{n} \times (\hat{n} \times \bar{E}) = -R\bar{J} \tag{5}$$

where

$$\bar{J} = [\hat{n} \times \bar{H}]_-^+ \tag{6}$$

is the total electric current supported. In recent years resistive sheets have been sucessfully employed in simulating a variety of dielectric structures. Diffraction effects have been studied analytically (see, for example, *Senior* [1979]) and, in addition, computer programs have been written to determine the field scattered by resistive strips and plates of arbitrary shape.

3.2. *Scattering by an infinite planar sheet*

The scattering properties of a resistive sheet are most easily understood by considering the simple problem of a plane wave incident on an infinite sheet lying in the plane $y = 0$ of a Cartesian coordinate system (x, y, z).

For the case of E polarization in which the incident electric vector is perpendicular to the xy plane of incidence, we assume

$$\bar{E}^i = \hat{z}e^{ik(x \sin\theta_0 - y\cos\theta_0)} \qquad (|\theta_0| \le \pi/2) \tag{7}$$

implying

$$\bar{H}^i = -Y(\hat{x}\cos\theta_0 + \hat{y}\sin\theta_0)e^{ik(x\sin\theta_0 - y\cos\theta_0)}$$

The reflected and transmitted electric vectors can be written as

$$\bar{E}^r = -\hat{z}\Gamma_E e^{ik(x\sin\theta_0 + y\cos\theta_0)}$$

and

$$\bar{E}^t = \hat{z}T_E e^{ik(x\sin\theta_0 - y\cos\theta_0)}$$

respectively, where Γ_E and T_E are constants still to be determined, and by applying the boundary con-

ditions (4)–(6), we obtain

$$\Gamma_E = \left(1 + \frac{2R}{Z}\cos\theta_0\right)^{-1} \tag{8}$$

$$T_E = \frac{2R}{Z}\cos\theta_0\,\Gamma_E \tag{9}$$

The current density $\bar{J}$ supported by the sheet is $\bar{J} = \hat{z}J_z$ with

$$J_z = 2Y\cos\theta_0\,\Gamma_E e^{ikx\sin\theta_0} \tag{10}$$

and recognizing that for a perfectly conducting sheet $\Gamma_E = 1$, it follows that

$$J_z = \Gamma_E J_z^{pc} \tag{11}$$

where the superscript pc refers to the perfectly conducting case.

The analysis for H polarization in which the incident magnetic vector is perpendicular to the plane of incidence is very similar. The reflection and transmission coefficients are

$$\Gamma_H = \left(1 + \frac{2R}{Z}\sec\theta_0\right)^{-1} \tag{12}$$

and

$$T_H = \frac{2R}{Z}\sec\theta_0\,\Gamma_H \tag{13}$$

respectively, and the current density $\bar{J}$ supported by the sheet is $\bar{J} = \hat{x}J_x$ with

$$J_x = 2\Gamma_H e^{ikx\sin\theta_0} \tag{14}$$

Thus

$$J_x = \Gamma_H J_x^{pc} \tag{15}$$

If $R \neq 0$, Γ_H decreases with increasing θ_0 and vanishes at grazing incidence ($\theta_0 = \pm\pi/2$).

3.3. *Scattering by a rectangular resistive plate*

As a simple model of a leaf we consider a rectangular resistive plate occupying the region $|x| \leq a/2$, $|z| \leq b/2$ of the plane $y = 0$, and seek the physical optics approximation to the bistatic scattered field. From the expressions (11) and (15) for the currents on an infinite sheet it is evident that the analysis is very similar to that for a perfectly conducting plate, and it is sufficient to summarize the derivation.

For E polarization in which the incident electric vector is (7), the physical optics approximation to the current induced in the plate is given in (10). Since only an electric current is supported, the scattered field can be attributed to the electric Hertz vector

$$\bar{\pi}(\bar{r}) = \hat{z}\,\frac{iZ}{4\pi k}\int_{-a/2}^{a/2}\int_{-b/2}^{b/2} J_z(x', z')\,\frac{e^{ik|\bar{r}-\bar{r}'|}}{|\bar{r}-\bar{r}'|}\,dx'\,dz'$$

where

$$\bar{r} = r(-\hat{x}\sin\theta + \hat{y}\cos\theta) \qquad \bar{r}' = \hat{x}x' + \hat{z}z'$$

and in the far field

$$\bar{\pi}(\bar{r}) = \hat{z}\,\frac{e^{ikr}}{kr}\,\frac{i}{2\pi}\,\Gamma_E\cos\theta_0\int_{-b/2}^{b/2}dz'\int_{-a/2}^{a/2} e^{ikx'(\sin\theta+\sin\theta_0)}\,dx'$$

$$= \hat{z}\,\frac{e^{ikr}}{kr}\,\frac{i}{2\pi}\,ab\cos\theta_0\,\Gamma_E\,\frac{\sin X}{X}$$

with

$$X = \frac{ka}{2}(\sin\theta + \sin\theta_0)$$

The scattered electric field is then

$$\bar{E}^s = \hat{z}\,\frac{e^{ikr}}{kr}\,S_E(\theta, \theta_0)$$

where the far-field amplitude is

$$S_E(\theta, \theta_0) = \frac{i}{2\pi}\,k^2ab\cos\theta_0\,\Gamma_E\,\frac{\sin X}{X} \tag{16}$$

In terms of the far-field amplitude the bistatic scattering cross section is

$$\sigma = \frac{\lambda^2}{\pi}|S|^2 \tag{17}$$

implying

$$\sigma_E(\theta, \theta_0) = 4\pi\left|\frac{ab}{\lambda}\cos\theta_0\,\Gamma_E\,\frac{\sin X}{X}\right|^2 \tag{18}$$

For H polarization in which the incident magnetic vector is in the z direction, the analysis is similar. The physical optics approximation to the current is (14), and in the far field the resulting electric Hertz vector is

$$\bar{\pi}(\bar{r}) = \hat{x}\,\frac{e^{ikr}}{kr}\,\frac{iZ}{2\pi}\,ab\,\Gamma_H\,\frac{\sin X}{X}$$

The scattered magnetic field is then

$$\bar{H}^s = \hat{z}\,\frac{e^{ikr}}{kr}\,S_H(\theta, \theta_0)$$

with

$$S_H(\theta, \theta_0) = -\frac{i}{2\pi} k^2 ab \cos\theta \, \Gamma_H \frac{\sin X}{X} \tag{19}$$

and the bistatic scattering cross section is

$$\sigma_H(\theta, \theta_0) = 4\pi \left| \frac{ab}{\lambda} \cos\theta \, \Gamma_H \frac{\sin X}{X} \right|^2 \tag{20}$$

In the backscattering direction ($\theta_0 = \theta$) the only polarization dependence is provided by the parameter Γ and

$$\sigma_{E,H}(\theta, \theta) = |\Gamma_{E,H}|^2 \sigma_{pc} \tag{21}$$

where σ_{pc} is the backscattering cross section of the perfectly conducting plate:

$$\sigma_{pc} = 4\pi \left\{ \frac{A}{\lambda} \cos\theta \frac{\sin(ka \sin\theta)}{ka \sin\theta} \right\}^2 \tag{22}$$

in which $A = ab$ is the plate area. In terms of the far-field amplitude $S(\theta, \theta_0)$ the extinction cross section is

$$\sigma^{ext} = \frac{\lambda^2}{\pi} \operatorname{Im} S(\theta, \theta + \pi) \tag{23}$$

and thus

$$\sigma^{ext}_{E,H} = 2A \cos\theta \operatorname{Re} \Gamma_{E,H} \tag{24}$$

We recognize $2A \cos\theta$ as the extinction cross section of a perfectly conducting plate of area A, and at normal incidence

$$\sigma^{ext}_E = \sigma^{ext}_H$$

4. COMPARISON WITH MEASURED DATA

In addition to the RCS of an actual leaf and a rectangular cutout, measurements were also made using a rectangular plate to gain confidence in the accuracy of the experimental procedures and the theoretical approximations. It is convenient to discuss them in the reverse order.

4.1. *Rectangular metal plate*

When a rectangular plate is illuminated with the direction of incidence in a principal plane, an approximate expression for the backscattered field can be obtained by treating the plate as a length b of an infinite strip or ribbon of width a. For a perfectly conducting strip, a uniform second order GTD expression for the bistatic scattered field has been developed by *Senior* [1979]. If the incident field is H polarized, the formula is equivalent to an asymptotic expansion of the uniform results of *Khaskind and Vainshteyn* [1964], and when specialized to the case of backscattering, the far-field amplitude of the plate is

$$\begin{aligned} S_H(\theta, \theta) = -\frac{kb}{4\pi \sin\theta} \Bigg\{ & (1 + \sin\theta) \left[1 - \frac{2}{\sqrt{\pi}} e^{-i\pi/4} \right. \\ & \left. \cdot \cos\left(\frac{\pi}{4} - \frac{\theta}{2}\right) F\left(\sqrt{2ka} \sin\left(\frac{\pi}{4} - \frac{\theta}{2}\right)\right) \right]^2 e^{ika \sin\theta} \\ & -(1 - \sin\theta) \left[1 - \frac{2}{\sqrt{\pi}} e^{-i\pi/4} \sin\left(\frac{\pi}{4} - \frac{\theta}{2}\right) \right. \\ & \left. \cdot F\left(\sqrt{2ka} \cos\left(\frac{\pi}{4} - \frac{\theta}{2}\right)\right) \right]^2 e^{-ika \sin\theta} \Bigg\} \end{aligned} \tag{25}$$

for $|\theta| \leq \pi/2$, where the phase origin has been chosen at the center of the plate and $F(x)$ is the Fresnel integral

$$F(x) = \int_x^\infty e^{i\mu^2} \, d\mu \tag{26}$$

We remark that S_H is finite and continuous for all θ including $\theta = 0$ corresponding to normal incidence, and in terms of S_H the backscattering cross section is given in (17).

In the case of E polarization, a similar approach applied to the uniform results of *Fialkovskiy* [1966] gives

$$\begin{aligned} S_E(\theta, \theta) = \frac{kb}{4\pi \sin\theta} \Bigg\{ & (1 - \sin\theta) \left[1 - \frac{2}{\sqrt{\pi}} e^{-i\pi/4} \right. \\ & \left. \cdot \cos^3\left(\frac{\pi}{4} - \frac{\theta}{2}\right) G\left(\sqrt{2\,ka} \sin\left(\frac{\pi}{4} - \frac{\theta}{2}\right)\right) \right]^2 e^{ika \sin\theta} \\ & -(1 + \sin\theta) \left[1 - \frac{2}{\sqrt{\pi}} e^{-i\pi/4} \sin^3\left(\frac{\pi}{4} - \frac{\theta}{2}\right) \right. \\ & \left. \cdot G\left(\sqrt{2\,ka} \cos\left(\frac{\pi}{4} - \frac{\theta}{2}\right)\right) \right]^2 e^{-ika \sin\theta} \Bigg\} \end{aligned} \tag{27}$$

[*Senior*, 1979], where

$$G(x) = F(x) - \frac{i}{2x} e^{ix^2} \tag{28}$$

In Figure 3 the theoretical expressions are compared with measured data for a plate having $b = 2\lambda$ and $a = 1.33\lambda$. Overall the agreement is excellent.

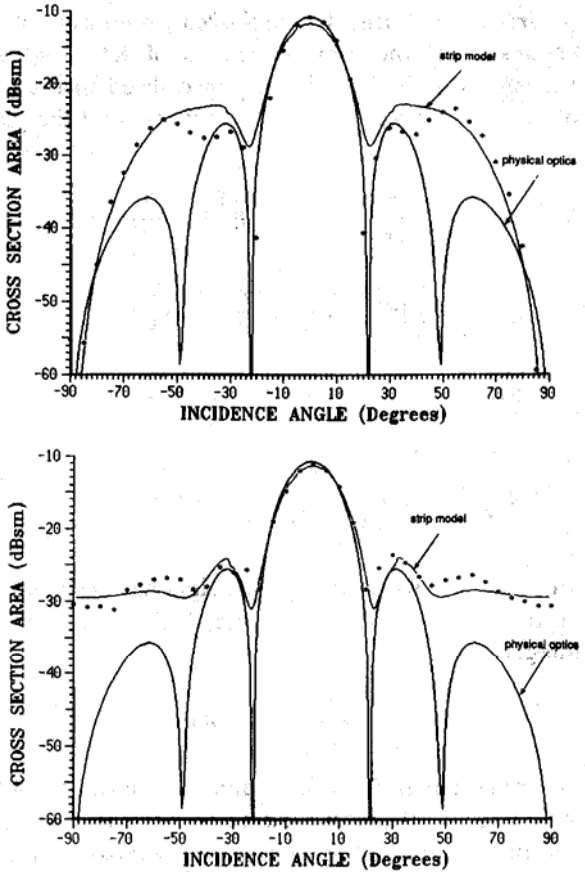

Fig. 3. The measured RCS (asterisks) of a thin metal plate ($a = 4$ cm, $b = 6$ cm) for (*a*) H polarization and (*b*) E polarization. The theoretical expressions (25) and (27) are much more accurate than the physical optics approximation (22).

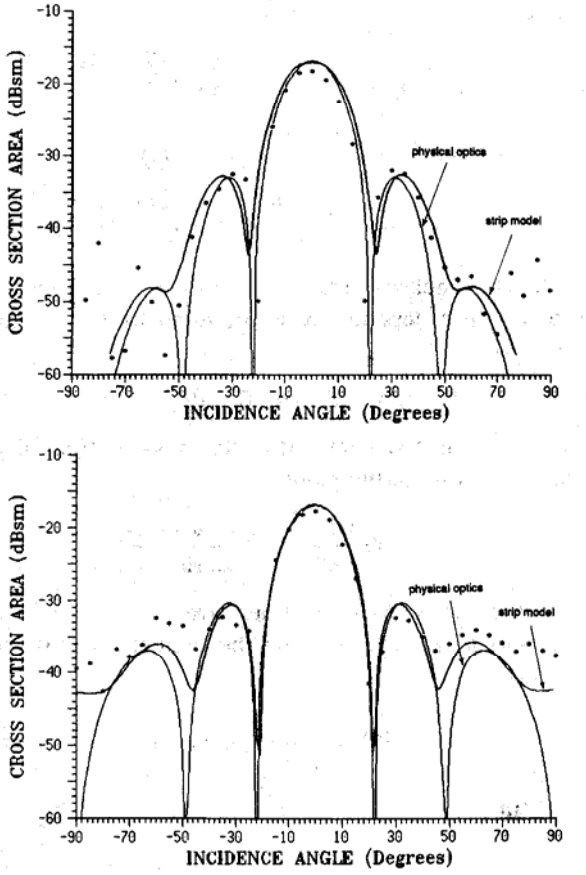

Fig. 4. The measured RCS (asterisks) of a rectangular section ($a = 4$ cm, $b = 6$ cm) of a freshly cut coleus leaf (Mg = 0.85) for (*a*) H polarization and (*b*) E polarization. The strip model provides very little improvement over the physical optics approximation (21).

With (25) used to compute σ_H, the strip model accurately reproduces the main features of the scattering pattern of a plate for H polarization, including the traveling wave lobes whose maxima occur at $\theta = \pm 54°$ and which override the outer side lobes of the specular flash. A similar agreement is found for E polarization, and the failure of (27) to reproduce the observed oscillation at angles close to grazing can be attributed to the effect of the currents borne by the side edges of the plate that are not accounted for by the strip model. The physical optics approximation (22) is included in Figure 3, and the improved accuracy provided by (25) and (27) is most evident at angles within (about) 45° from grazing.

4.2. *Rectangular resistive plate*

For a rectangular plate of uniform resistivity R, formulas analogous to (25) and (27) can be derived from the GTD expression for the bistatic scattered field of a resistive strip [*Senior*, 1979; *Herman and Volakis*, 1987], but as the resistivity increases, the improvement over the physical optics formula for a resistive plate diminishes. Even a resistivity as low as 20 ohms per square effectively eliminates the traveling wave lobe for H polarization [*Senior*, 1985] and exposes the underlying side lobes of the specular flash. Similarly, for E polarization, the resistivity reduces the strong edge effects, including the influence of the side edges of the plate.

The net result is to improve the accuracy of the physical optics approximation (21), and this is illustrated in Figure 4, where the measured data for a rectangular leaf are compared with the strip model [*Herman and Volakis*, 1987] and physical optics. The rectangle was cut from a fresh coleus leaf having Mg = 0.85, and the (complex) resistivity was com-

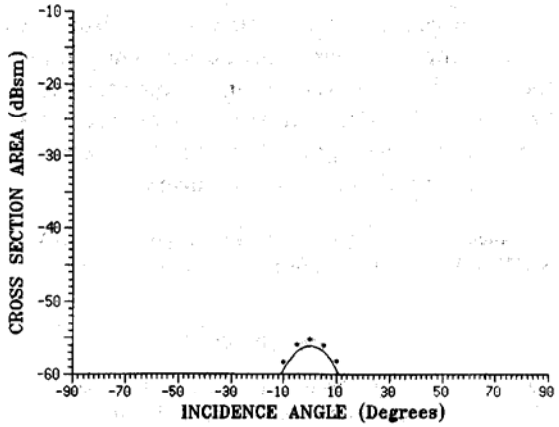

Fig. 5. The measured RCS (asterisks) of the dried leaf section (Mg = 0) compared with the physical optics approximation (21) for E polarization. The results for H polarization are the same.

puted from (3) using (1) and (2). The only significant differences between the strip and physical optics formulas occur for incidence angles within a few degrees of grazing, and the physical optics approximation is in good agreement with the measured data over most of the angular range. Similar agreement was found for other moisture contents, and Figure 5 shows the results for a dried leaf having Mg = 0. Even at this low level of reflectivity the physical optics approximation (21) retains its accuracy, and the dynamic range is illustrated in Figure 6.

4.3. *Natural leaf*

In the light of the above results it was anticipated that the physical optics approximation applied to the resistive sheet model would provide a good approximation to the RCS of an actual leaf at most angles of incidence. To test this, measurements were made using a coleus leaf whose area was $A = 39.5$ cm^2. The width of the equivalent rectangle was chosen as 5.6 cm, implying $b = 7.1$ cm, and the measured RCS of the freshly cut leaf (Mg = 0.77) is compared with the physical optics approximation (21) in Figure 7. In view of the obvious uncertainty in the specification of a (or b), the agreement is good down to at least 20 dB below the broadside peak. Similar agreement was found for the same leaf with Mg = 0.85, 0.62, and 0.04.

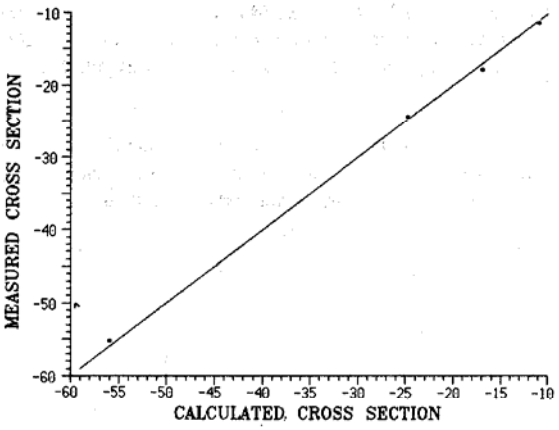

Fig. 6. The measured RCS (asterisks) of the leaf section for various moisture contents at normal incidence are in excellent agreement with the physical optics values. The 1 : 1 line is shown.

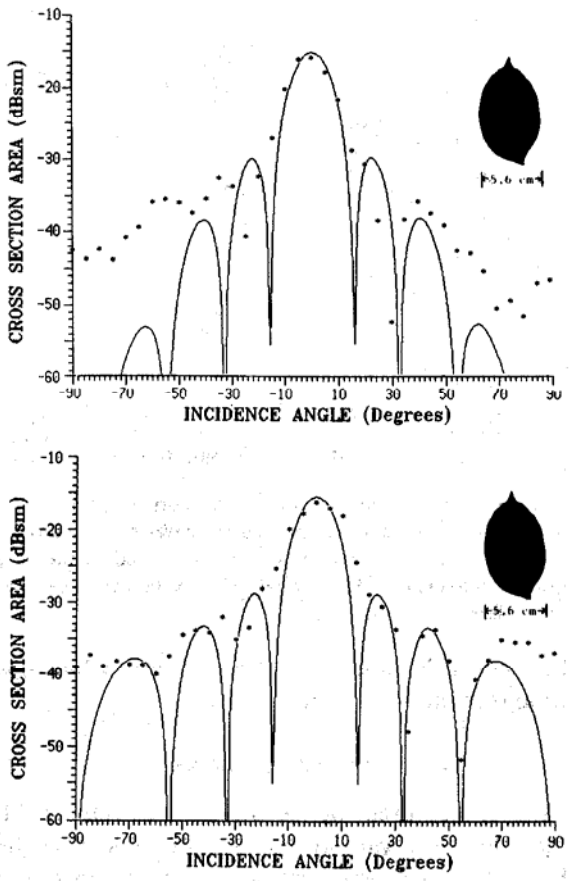

Fig. 7. The measured RCS (asterisks) of a natural coleus leaf having $A = 39.5$ cm^2 and Mg = 0.77 for (*a*) H polarization and (*b*) E polarization, compared with the physical optics approximation (21) assuming $a = 5.6$ cm.

The theoretical extinction and backscattering cross sections (24) and (21) respectively, normalized to their perfectly conducting values, are plotted as functions of the moisture content Mg for normal incidence ($\theta = 0$) in Figure 8. The measured values of σ/σ_{pc} for

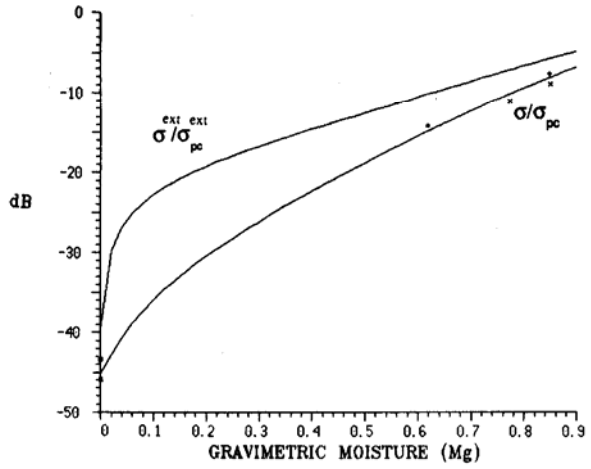

Fig. 8. The measured values of the normalized RCS of rectangular (asterisks) and natural (pluses) leaves as functions of Mg at normal incidence are accurately approximated by the physical optics expression (21). The normalized extinction cross section (24) is also shown.

the rectangular and natural leaves are included, and the agreement is excellent.

5. CONCLUSIONS

Using measurements of the backscattered field of coleus leaves in varying stages of dryness, it has been shown that a resistive sheet constitutes an effective model of a leaf. The resistivity is entirely specified by the moisture content, and for a rectangular section of a leaf, the predicted backscattering cross sections are in excellent agreement with the measured data for both principal polarizations, including the special case of a rectangular metal plate whose resistivity is zero. As the resistivity increases, the effect of the currents borne by the edges of the plate diminishes, and the accuracy of the physical optics approximation improves. Indeed, for a natural leaf, the physical optics approximation in conjunction with the resistive sheet model faithfully reproduces the dominant features of the scattering patterns for all of the moisture conditions investigated, representing a dynamic range of more than 50 dB. The simplicity of the formulation is such that the bistatic and extinction cross sections can also be computed, and the aspect angle averaging that may be necessary in a practical situation is easily performed.

Acknowledgment. This work was supported by NASA grant NAG5-480, NASA/GSFC, Beltsville, Maryland.

REFERENCES

Fialkovskiy, A. T., Diffraction of planar electromagnetic waves by a slot and a strip, *Radio Eng. Electron.*, *11*, 150–157, 1966.

Harrington, R. F., and J. R. Mautz, An impedance sheet approximation for thin dielectric shells, *IEEE Trans. Antennas Propag.*, *23*, 531–534, 1975.

Herman, M. I., and J. L. Volakis, High-frequency scattering by a resistive strip and extensions to conductive and impedance strips, *Radio Sci.*, *22*, 335–349, 1987.

Khaskind, M. D., and L. A. Vainshteyn, Diffraction of plane waves by a slit and a tape, *Radio Eng. Electron.*, *9*, 1492–1502, 1964.

Lang, R. H., Electromagnetic backscattering from a sparse distribution of lossy dielectric scatterers, *Radio Sci.*, *16*, 15–30, 1981.

LeVine, D. M., R. Meneghini, R. H. Lang, and S. S. Seker, Scattering from arbitrarily oriented dielectric disks in the optics region, *J. Opt. Soc. Am.*, *73*, 1255–1262, 1983.

LeVine, D. M., A. Snyder, R. H. Lang, and H. G. Carter, Scattering from thin dielectric disks, *IEEE Trans. Antennas Propag.*, *33*, 1410–1413, 1985.

Senior, T. B. A., Scattering by resistive strips, *Radio Sci.*, *14*, 911–924, 1979.

Senior, T. B. A., Scattering by resistive strips and plates, *Rep. 388919-1-F*, Univ. of Mich. Radiat. Lab., Ann Arbor, Mich., 1985.

Tsang, L., J. A. Kong, and R. T. Shin, Radiative transfer theory for active remote sensing of a layer of nonspherical particles, *Radio Sci.*, *19*, 629–642, 1984.

Ulaby, F. T., and M. El-Rayes, Microwave dielectric spectrum of vegetation material, paper presented at Geoscience Remote Sensing Symposium, IEEE, Zurich, Switzerland, Sept. 8–11, 1986.

K. Sarabandi, T. B. A. Senior, and F. T. Ulaby, Radiation Laboratory, Electrical Engineering and Computer Science Department, University of Michigan, Ann Arbor, MI 48109.